Journal of Alloys and Compounds, 207/208 (1994) 213–220
JALCOM 3009

Interpretation of the magnetic specific heat of oxygen deficient and doped $NdBa_2Cu_3O_x$ and $DyBa_2Cu_3O_x$ compounds

P. Allenspach* and M.B. Maple
Institute for Pure and Applied Physical Sciences and Department of Physics, University of California, San Diego, La Jolla, CA 92093-0075 (USA)

A. Furrer
Laboratory for Neutron Scattering, ETH Zurich, 5232 Villigen PSI (Switzerland)

Abstract

In contrast to $NdBa_2Cu_3O_x$ samples with x close to 7 and 6 which according to neutron diffraction and specific heat measurements exhibits long-range antiferromagnetic ordering of the Nd^{3+} ions, only short-range magnetic ordering has been found in the intermediate oxygen range $6.9 \gtrsim x \gtrsim 6.6$. The short-range ordering behavior of the magnetic specific heat is neither of one-dimensional chain-type nor two-dimensional XY or Heisenberg type, but could be explained by two-dimensional Heisenberg spin-1/2 clusters. A two-dimensional Ising cluster model was applied to $DyBa_2Cu_3O_x$ in order to account for the high single ion anisotropy of Dy^{3+}; this model reproduces the zero magnetic field specific heat data but does not agree as well as the Heisenberg model with the data taken in an external magnetic field.

1. Introduction

The replacement of Y^{3+} ions in the compound $YBa_2Cu_3O_7$ (Y1237) by rare earth R^{3+} ions (forming R1237) has, except for R = Pr, hardly any effect on the superconducting transition temperature T_c, despite the occurrence of long-range magnetic ordering of the R^{3+} ions in some of these compounds at temperatures of the order of 1 K. The relative isolation of the 4f electrons of the rare earth ions from the CuO_2 superconducting layers is believed to be the reason for the co-existence of superconductivity and long-range magnetic ordering. A reduction of the oxygen content x in R123x (and in Y123x) results in a reduction of T_c which is dependent on the type of substituted rare earth [1]. For the compounds with small rare earth ions (Gd, Dy, Ho, Er, Tm, Yb), the behavior of T_c versus oxygen content x coincides with that of the Y123x compound, whereas for the compounds with large rare earth ions (La, Nd, Sm, Eu), the "two-plateau" behavior of $T_c(x)$ is less pronounced and superconductivity disappears at higher oxygen content (the larger the R ion, the faster superconductivity is destroyed). It is tempting to attribute this dependence of T_c on the type of rare earth ion to different amounts of overlap between the 4f electron wave functions and the wave functions of the surrounding O and Cu ions. Investigations of the magnetic ordering as a function of rare earth ion and oxygen content should reveal a strong dependence of the magnetic ordering on the amount of overlap, if superexchange is the main interaction, and almost no effect, if the dipolar interaction is dominant.

In the present work, we have concentrated on the compounds $NdBa_2Cu_3O_x$ and $DyBa_2Cu_3O_x$. The magnetic ordering in both systems has been studied extensively by means of heat capacity [2–8] and neutron diffraction [9–15] measurements. For $NdBa_2Cu_3O_x$ samples with x very close to 7, long-range antiferromagnetic ordering was observed by means of both methods. However, while neutron scattering indicates three-dimensional (3D) ordering with the magnetic moments directed along the c-axis [9], the anomaly in the magnetic contribution to the specific heat; is best described by an anisotropic two-dimensional (2D) Ising model (see Fig. 1 and Ref. 2). This indicates that although the ordering is 3D, its character is mainly 2D. By reducing the oxygen content, T_N shifts to slightly lower temperatures and the sharp peak becomes smaller and broader. For $x < 6.9$, there is no longer any indication of long-range magnetic ordering in the heat capacity data. Also, neutron diffraction measurements on a sample with $x = 6.78$ do not reveal any long-range ordering [15]. By reducing the oxygen content further,

*Present address: Laboratory for Neutron Scattering, ETH Zurich, 5232 Villigen PSI, Switzerland.

0925-8388/94/$07.00
SSDI 0925-8388(93)03009-8

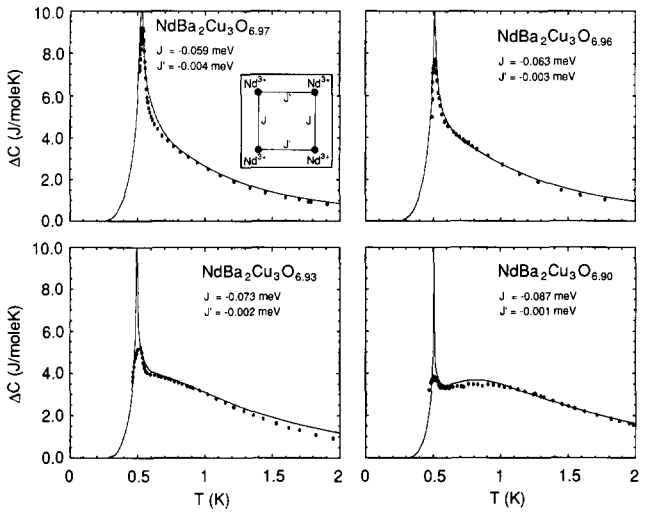

Fig. 1. Magnetic specific heat data for Nd123x samples for several values of $x \geqslant 6.9$ and 2D-Ising fits. The exchange integrals are defined as shown in the inset. After Ref. 6.

the broad peak in the specific heat, already observed on the high temperature side of the sharp peak for samples with long-range magnetic ordering, increases and shifts continuously to higher temperatures. After crossing the metal-insulator (superconducting-non-superconducting) transition at about 6.6, long-range antiferromagnetic ordering (most likely 3D Ising) gradually develops again [4].

Substituting Ba partially by Nd in $NdBa_2Cu_3O_7$ yields a similar behavior of the specific heat as in oxygen reduced samples with a comparable density of charge carriers in the CuO_2 planes ($Nd_{1.25}Ba_{1.75}Cu_3O_7$ corresponds to $NdBa_2Cu_3O_{6.72}$ and $Nd_{1.5}Ba_{1.5}Cu_3O_7$ to $NdBa_2Cu_3O_{6.64}$, respectively). Reduction of both of these doped samples to an oxygen content of 6.50 and 6.55, respectively, results in the same kind of 3D Ising type specific heat anomaly as observed for $NdBa_2Cu_3O_{6.26}$ [7]. It is remarkable that non-superconducting $Nd_{1.5}Ba_{1.5}Cu_3O_7$ displays the same behavior of the specific heat as superconducting $NdBa_2Cu_3O_{6.64}$. This shows that the appearance of the long-range magnetic ordering between 6.5 and 6.3 is not triggered by the metal-insulator (M-I) transition but more likely by the magnetic ordering of the Cu ions. Whereas in the undoped Nd123x, the appearance of the Cu ordering coincides with the M-I transition, there is no crossing of an M-I transition in $Nd_{1.5}Ba_{1.5}Cu_3O_x$. Nevertheless, a change in the Cu ordering was observed in $Nd_{1.5}Ba_{1.5}Cu_3O_x$ between $x=6.88$ and $x=6.39$. In the sample with the lower oxygen content, the Cu ordering and the spin reorientation are comparable to that of undoped deoxygenated Nd123x, but in the sample with the higher oxygen content, no spin reorientation takes place [16].

The behavior of the magnetic specific heat of $DyBa_2Cu_3O_x$ as a function of oxygen content is very similar to that of $NdBa_2Cu_3O_x$ long-range antiferromagnetic ordering (2D-Ising) at high oxygen content, a decrease and broadening of the magnetic anomaly at reduced oxygen content, culminating in short-range interactions for $DyBa_2Cu_3O_{6.34}$ which is still superconducting, and in the non-superconducting regime, a reappearance of sharpness and strength of the magnetic anomaly, indicative of a increasing correlation length. The main difference between the two compounds is the position of the peak; whereas it shifts strongly in $NdBa_2Cu_3O_x$, it hardly moves in $DyBa_2Cu_3O_x$ (Fig. 2).

In the present paper, we try to shed light on the question of the type of short-range magnetic interaction in the intermediate oxygen range in the $RBa_2Cu_3O_x$ (R = Nd, Dy) compounds. As shown in Fig. 3, the 1D- (Ising, Heisenberg and XY) and the 2D- (Heisenberg and XY) models are not able to explain the behavior of the magnetic specific heat. If the 2D-Heisenberg model had been appropriate, the question about the mechanism behind the transition to short-range interactions would have been very easy to answer. According to crystalline electric field (CEF) calculations of the

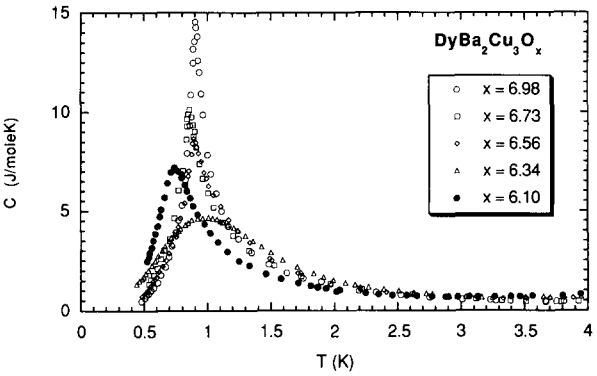

Fig. 2. Specific heat data for Dy123x as a function of the oxygen content. From Refs. 1–5, 8.

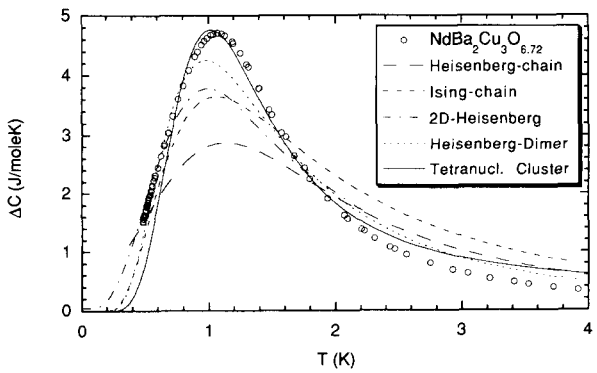

Fig. 3. Specific heat data for $NdBa_2Cu_3O_{6.72}$ (from Ref. 8) and fits of several different models.

magnetic properties of $NdBa_2Cu_3O_x$, the c-axis is the easy axis of magnetization for $x > 6.9$, whereas between 6.9 and 6.6, the system becomes isotropic (for $x < 6.6$, the easy axis is the a-axis). Thus, if for very high oxygen content, 2D-Ising long-range ordering was found, for oxygen content between 6.9 and 6.6, a 2D-Heisenberg-type behavior (without long-range ordering at finite temperatures) would have been expected. But this is not the case, as clearly shown in Fig. 3. We believe that only a cluster approach is able to explain the data.

2. Model

The first excited Kramers doublet for Nd^{3+} in Nd123x lies above the ground state 11–12 meV (depending on the oxygen content [17]), high enough not to significantly influence the ground state doublet in the temperature range investigated in the present work. Therefore, Nd^{3+} can be treated at low temperatures as an effective spin-1/2 system.

Since the single ion anisotropy of the Nd compound is rather small in an intermediate range of oxygen content, a Heisenberg cluster model was chosen to be compared with the specific heat data. This choice is supported by the fact that the magnetic heat capacity of an antiferromagnetic Heisenberg spin-1/2 dimer closely resembles the heat capacity data, whereas the Ising spin-1/2 dimer model clearly fails to reproduce the data [18].

A constraint on the cluster approach is the amount of entropy change due to magnetic interactions of the rare earth ions. The measured entropy change for Nd123x is always very close to $R\ln(2)$, as expected for a doublet system [8] (the slight increase in entropy as a function of decreasing oxygen content is most likely due to interactions with the Cu ions). The interaction of n magnetic ions results in a sequence of $(2s+1)^n$ energy levels (in our case with $s = 1/2$:2^n). The entropy change in such a multi-level system can be calculated to be

$$\Delta S = R \ln\left(\frac{t}{g}\right) \tag{1}$$

where t is the total number of energy levels and g is the degeneracy of the ground state. In a Heisenberg model, g is odd for an even number, and even for an odd number of magnetic ions. Hence, the maximum entropy change per mole of magnetic ions is:

$$\Delta S = \frac{1}{n} R \ln(2^n) = R \ln(2), \quad n \text{ even} \tag{2}$$

$$\Delta S = \frac{1}{n} R \ln\left(\frac{2^n}{2}\right) = \left(1 - \frac{1}{n}\right) R \ln(2), \quad n \text{ odd} \tag{3}$$

Equation (3) shows that the entropy change calculated for an odd number of magnetic ions only reaches the measured value for large clusters (a cluster of at least 25 ions is needed for an experimental error of about 4% in the entropy). Neutron diffraction data indicate that the magnetic correlation lengths in these samples are of the order of 20 Å which is roughly equivalent to 5 unit cells (and ~ 25 Nd^{3+} ions) [14]. Thus, clusters with an even as well as an odd number of magnetic ions may contribute to the observed specific heat, but approximations must be made for a quantitative investigation in order to reduce the complexity of the calculation. First, the number of magnetic ions was kept fixed for the whole temperature range and, second, the smallest cluster able to reproduce the measured data was used for the calculations. Of course, both assumptions are gross simplifications of the real behavior of these systems. Upon cooling down from high temperature, magnetic dimers will nucleate at a certain temperature, followed by the formation of larger and larger magnetic clusters at successively lower temperatures, finally resulting in clusters of the size measured by neutron diffraction at very low temperatures. The smallest cluster that describes the specific heat data sufficiently well is a cluster consisting of four magnetic ions coupled by three different exchange interactions defined by $J = J_{12} = J_{34}$, $J' = J_{23} = J_{14}$ and $J = J_{13} = J_{24}$ (Fig. 4).

The irreducible tensor method used to calculate the eigenvalues of tetranuclear magnetic clusters was developed by Fano and Racah [19] and Wigner [20]. Considering only two-body interactions and $S_1 = S_2 = S_3 = S_4 = 1/2$, the exchange Hamiltonian is given by

$$\hat{\mathbf{H}}_{ex} = \sum_{i>j} a(i,j)\hat{\mathbf{S}}_i \cdot \hat{\mathbf{S}}_j \tag{4}$$

where $\hat{\mathbf{S}}$ is a spin operator and $a(i,j) = 2S_1(S_1+1)(2S_1+1)J_{ij} = 3J_{ij}$, which includes the bilinear exchange parameter J_{ij} [21]. The appropriate basis states of a system with four spins S_i coupled to a resultant S are of the form $|S_{12}S_{34}SM\rangle$ (*i.e.* two singlets $|0000\rangle$ and $|1100\rangle$, three triplets $|101M\rangle$, $|011M\rangle$, and $|111M\rangle$, and one quintet $|112M\rangle$) with $\mathbf{S}_{12} = \mathbf{S}_1 + \mathbf{S}_2$ and $\mathbf{S}_{34} = \mathbf{S}_3 + \mathbf{S}_4$. The matrix elements of the Hamiltonian (eqn. (4)) are considered separately for each of the six possible (i,j) pairs [21]:

$$\begin{aligned}\langle S_{12}S_{34}SM|\hat{\mathbf{S}}_1 \cdot \hat{\mathbf{S}}_2|S'_{12}S'_{34}SM\rangle &= \delta(S_{12},S'_{12})\delta(S_{34},S'_{34})(-1)^{S_1+S_2+S_{12}+k} \\ &\times \begin{Bmatrix} S_1 & S_1 & k \\ S_2 & S_2 & S_{12} \end{Bmatrix}\end{aligned} \tag{5}$$

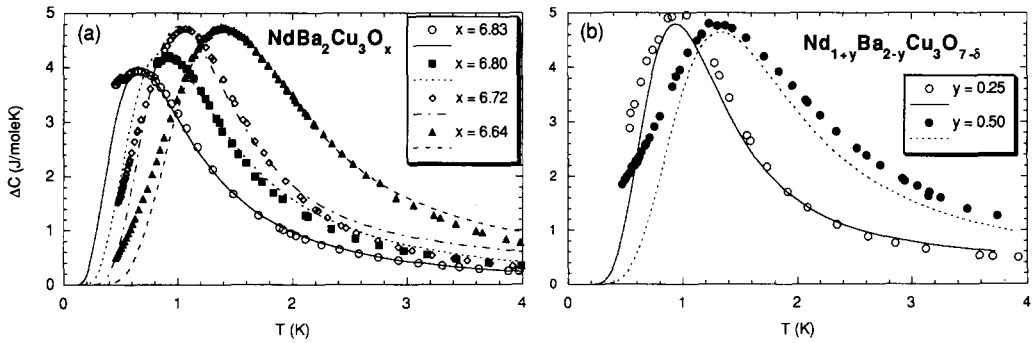

Fig. 4. Specific heat data for Nd123x and $Nd_{1+y}Ba_{2-y}Cu_3O_7$ samples (taken from Ref. 7). The parameters of the tetranuclear cluster fits are displayed in Table 1 and Fig. 6. The definition of the tetranuclear Heisenberg cluster is shown in the inset. The fits for $Nd_{1+y}Ba_{2-y}Cu_3O_7$ are much worse than that for Nd123x, most likely due to magnetic interactions of the Nd^{3+} ions at the Ba sites.

$$\langle S_{12}S_{34}SM|\hat{\mathbf{S}}_3\cdot\hat{\mathbf{S}}_4|S'_{12}S'_{34}SM\rangle = \delta(S_{12},S'_{12})\delta(S_{34},S'_{34})(-1)^{S_3+S_4+S_{34}+k} \times \begin{Bmatrix} S_3 & S_3 & k \\ S_4 & S_4 & S_{34} \end{Bmatrix} \tag{6}$$

$$\langle S_{12}S_{34}SM|\hat{\mathbf{S}}_1\cdot\hat{\mathbf{S}}_3|S'_{12}S'_{34}SM\rangle = (-1)^{S_1+S_2+S_3+S_4+2S'_{12}+S_{34}+S'_{34}+S+k} \times\sqrt{(2S_{12}+1)(2S'_{12}+1)(2S_{34}+1)(2S'_{34}+1)} \times \begin{Bmatrix} S_{12} & S_{34} & S \\ S'_{34} & S'_2 & k \end{Bmatrix}\begin{Bmatrix} S_{12} & S'_{12} & k \\ S_1 & S_1 & S_2 \end{Bmatrix}\begin{Bmatrix} S_{34} & S'_{34} & k \\ S_3 & S_3 & S_4 \end{Bmatrix} \tag{7}$$

$$\langle S_{12}S_{34}SM|\hat{\mathbf{S}}_1\cdot\hat{S}_4|S'_{12}S'_{34}SM\rangle = (-1)^{S_{34}-S'_{34}}\langle S_{12}S_{34}SM|\hat{\mathbf{S}}_1\cdot\hat{\mathbf{S}}_3|S'_{12}S'_{34}SM\rangle \tag{8}$$

$$\langle S_{12}S_{34}SM|\hat{\mathbf{S}}_2\cdot\hat{\mathbf{S}}_3|S'_{12}S'_{34}SM\rangle = (-1)^{S_{12}-S'_{12}}\langle S_{12}S_{34}SM|\hat{\mathbf{S}}_1\cdot\hat{\mathbf{S}}_3|S'_{12}S'_{34}SM\rangle \tag{9}$$

$$\langle S_{12}S_{34}SM|\hat{\mathbf{S}}_2\cdot\hat{\mathbf{S}}_4|S'_{12}S'_{34}SM\rangle = (-1)^{S_{12}-S'_{12}+S_{34}-S'_{34}}\langle S_{12}S_{34}SM|\hat{\mathbf{S}}_1\cdot\hat{\mathbf{S}}_3|S'_{12}S'_{34}SM\rangle \tag{10}$$

The specific heat was calculated from the resulting eigenvalues according to the standard multi-level Schottky formula

$$C(T) = \frac{R}{Z}\left[\sum_n\left(\frac{E_n}{k_BT}\right)^2\rho_n - \frac{1}{Z}\left(\sum_n\frac{E_n}{k_BT}\rho_n\right)^2\right] \tag{11}$$

with

$$\rho_n = \exp\left(\frac{-E_n}{k_BT}\right) \quad \text{and} \quad Z = \sum_n\rho_n \tag{12}$$

A magnetic field parallel to the c-axis was introduced by adding a Zeeman term to the Hamiltonian (eqn. (4)) and, subsequently, diagonalizing the matrix with these additional terms.

For Dy123x, the same procedure was used, despite the fact that the first exited CEF doublet lies only 3.3 meV (38 K) above the ground state doublet. Therefore, admixture effects may play a role, but were neglected in this work. In addition, for Dy^{3+} with its very high single ion anisotropy in Dy123x ($g_z \gg g_x, g_y$, [22]), a 2D-Ising cluster model was also used. The cluster was again chosen to be as small as possible, but large enough to satisfy the entropy condition. The entropy change in $DyBa_2Cu_3O_{6.34}$ was measured to be slightly less than $0.9R\ln(2)$. Since the levels are at least doubly degenerate (opposite spin arrangements have the same energy in zero magnetic field in the Ising model), eqn. (3) has to be applied and the entropy condition is fulfilled with at least nine magnetic ions. The coupling between these ions is shown in the inset of Fig. 5. The Hamiltonian can then be written as

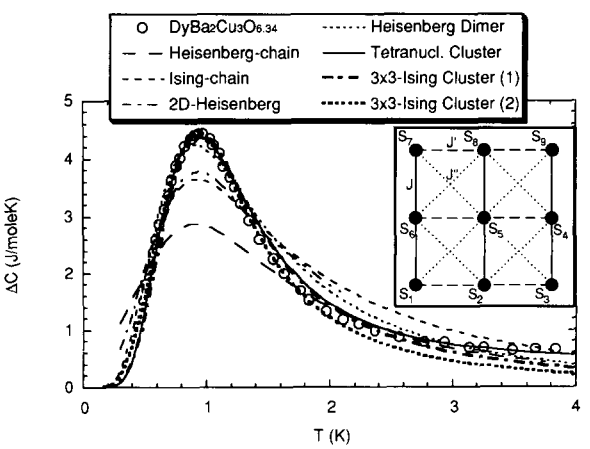

Fig. 5. Specific heat data for $DyBa_2Cu_3O_{6.34}$ together with fits of several different models. The definition of the 3×3-Ising cluster is shown in the inset.

$$\hat{\mathbf{H}} = \sum_{\text{all spin config.}} \Big[-2J(S_{z1}S_{z2} + S_{z2}S_{z3} + S_{z4}S_{z5} + S_{z6}S_{z7} + S_{z7}S_{z8} + S_{z8}S_{z9}) - 2J'(S_{z1}S_{z6} + S_{z6}S_{z7} + S_{z2}S_{z5} + S_{z5}S_{z8} + S_{z3}S_{z4} + S_{z4}S_{z9}) - 2J''(S_{z1}S_{z5} + S_{z2}S_{z6} + S_{z2}S_{z4} + S_{z3}S_{z5} + S_{z6}S_{z8} + S_{z5}S_{z7} + S_{z5}S_{z9} + S_{z4}S_{z8}) - g\mu_B H_z \sum_{i=1}^{9} S_{zi} \Big] \quad (13)$$

With the help of the resulting 512 (2^9) eigenvalues, the specific heat was again calculated using eqn. (11).

3. Results and discussion

Fits of the models to the data from Ref. 8 are shown in Fig. 4 for Nd123x and Fig. 5 for Dy123x, respectively. Despite slight deviations at very low and high temperatures, the theoretical curves reproduce the data quite well. The only question is whether the parameters obtained are physically reasonable.

Figure 6 displays the behavior of the exchange integrals for Nd123x as a function of x. The four parameter pairs for a high oxygen content were taken from the anisotropic 2D-Ising fits shown in Fig. 1; the rest are

TABLE 1. Exchange integrals for Nd123x and $Nd_{1+y}Ba_{2-y}Cu_3O_7$ samples in meV

	J	J'	J''
$NdBa_2Cu_3O_{6.97}$	-0.057 ± 0.005	-0.004 ± 0.001	0.000
$NdBa_2Cu_3O_{6.96}$	-0.063 ± 0.005	-0.003 ± 0.001	0.000
$NdBa_2Cu_3O_{6.93}$	-0.073 ± 0.006	-0.002 ± 0.001	0.000
$NdBa_2Cu_3O_{6.90}$	-0.087 ± 0.008	-0.001 ± 0.001	0.000
$NdBa_2Cu_3O_{6.83}$	-0.080 ± 0.013	0.045 ± 0.014	0.005 ± 0.014
$NdBa_2Cu_3O_{6.80}$	-0.110 ± 0.015	0.055 ± 0.015	0.027 ± 0.016
$NdBa_2Cu_3O_{6.72}$	-0.156 ± 0.019	0.161 ± 0.020	0.139 ± 0.020
$NdBa_2Cu_3O_{6.64}$	-0.205 ± 0.022	0.178 ± 0.021	0.168 ± 0.022
$Nd_{1.25}Ba_{1.25}Cu_3O_7$	-0.147 ± 0.035	0.147 ± 0.041	0.147 ± 0.039
$Nd_{1.5}Ba_{1.5}Cu_3O_7$	-0.187 ± 0.038	0.139 ± 0.040	0.125 ± 0.041

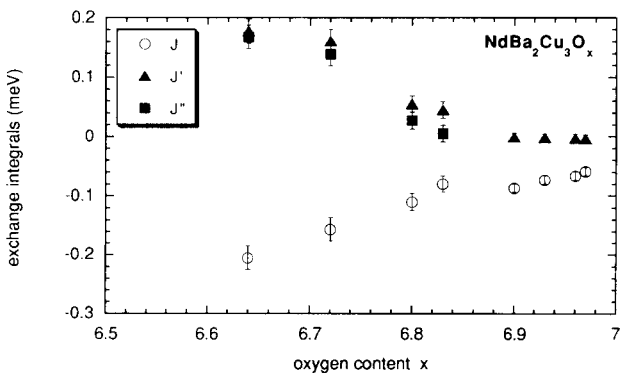

Fig. 6. Exchange integrals versus oxygen content x for Nd123x.

the results of the 2D Heisenberg spin-1/2 cluster fits. The Hamiltonian in eqn. (4) is symmetric in the exchange integrals J' and J''; therefore, it cannot be decided which of the two corresponds to J' in the 2D-Ising model. As can be seen in Fig. 6, the trend of J' to go to positive values for the samples with $x > 6.9$ is continued in the more oxygen deficient samples. Antiferromagnetic coupling in one direction and ferromagnetic in the other was observed in $HoBa_2Cu_3O_7$ (ferromagnetic coupling in the b-direction [23]) and is therefore not totally surprising. Another indication of ferromagnetic coupling is provided by an upturn below T_N in magnetic susceptibility data [24]. The Curie–Weiss temperature obtained from a fit to these data yields $\theta = 0.7$ K, very close to the value obtained from the exchange integrals in the present work (0.8 K). More surprising is the size of the diagonal exchange integral (either J' or J''), which would be expected to be rather small in this geometrical configuration. Most likely, this is an artifact of the limitation to a fixed cluster size.

No systematic study of the development of the exchange integrals by decreasing the oxygen content is possible for Dy123x. The shape of the magnetic anomalies for samples with $6.8 < x < 6.4$ and for $DyBa_2Cu_3O_{6.10}$ cannot be explained with any of the models presented here, but resembles very much the specific heat resulting from large 2D-Ising clusters displayed in Fig. 3 of Ref. 25. The decay of the long-range magnetically ordered 2D-Ising system into smaller and smaller 2D-Ising clusters with a minimum at $x = 6.34$ (3×3-cluster) would be a straightforward explanation for the behavior of the specific heat as a function of oxygen. Again, the increase in cluster size in the semiconducting regime may be due to the Cu ordering.

A test for all these assumptions is provided by heat capacity measurements in an external magnetic field for $NdBa_2Cu_3O_{6.80}$ (Fig. 7(a)), $NdBa_2Cu_3O_{6.64}$ (Fig. 8(a)), and $DyBa_2Cu_3O_{6.34}$ (Fig. 9(a)). The corresponding CEF calculations (data taken from Refs. 17, 22) of the splitting of the ground state doublet in the absence of magnetic interactions are shown in Figs. 7(b), 8(b) and 9(b), respectively. It can be clearly seen that for sufficiently high magnetic fields (4 T for Nd123x and 2 T for Dy123x), the specific heat anomalies evolve into single ion behavior. In smaller fields, a decrease in the maximum with no big changes in the position of the anomaly was observed for all three samples. By further increasing the magnetic field, the anomaly shifts to higher temperatures and the maximum begins to increase slightly. A similar magnetic field dependence is found for the 2D-Heisenberg cluster model (Figs. 7(c), 8(c) and 9(c)), but the decrease in the maximum of the specific heat is more pronounced. The reason for this is the crossing of the ground state singlet by an excited singlet in a magnetic field

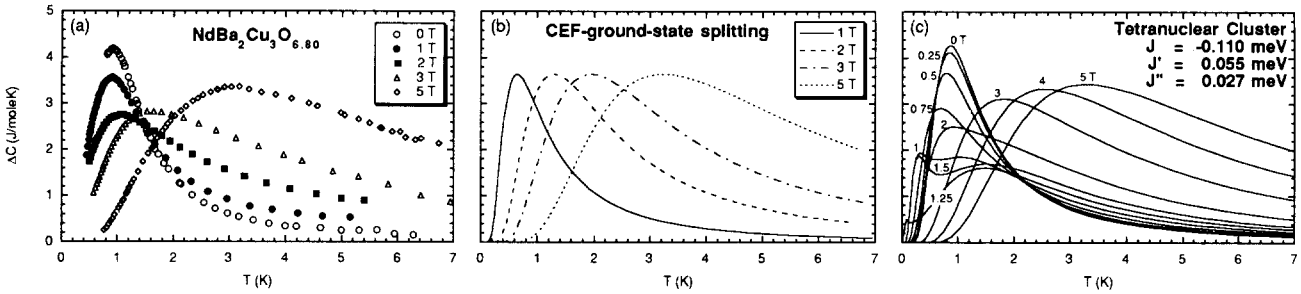

Fig. 7. (a) Specific heat data for $NdBa_2Cu_3O_{6.80}$ in different external magnetic fields (field-cooled data from Ref. 8); (b) calculations of the splitting of the CEF ground state doublet in different magnetic fields; and (c) calculations of the magnetic field behavior of a tetranuclear Heisenberg cluster.

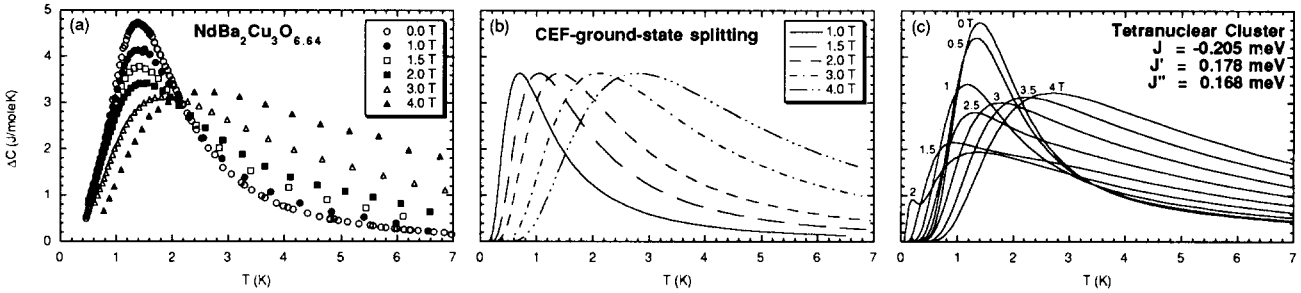

Fig. 8. (a) Specific heat data for $NdBa_2Cu_3O_{6.64}$ in different external magnetic fields (zero-field cooled data from Ref. 8); (b) calculation of the splitting of the CEF ground state doublet in different magnetic fields, and (c) calculation of the magnetic field behavior of a tetranuclear Heisenberg cluster.

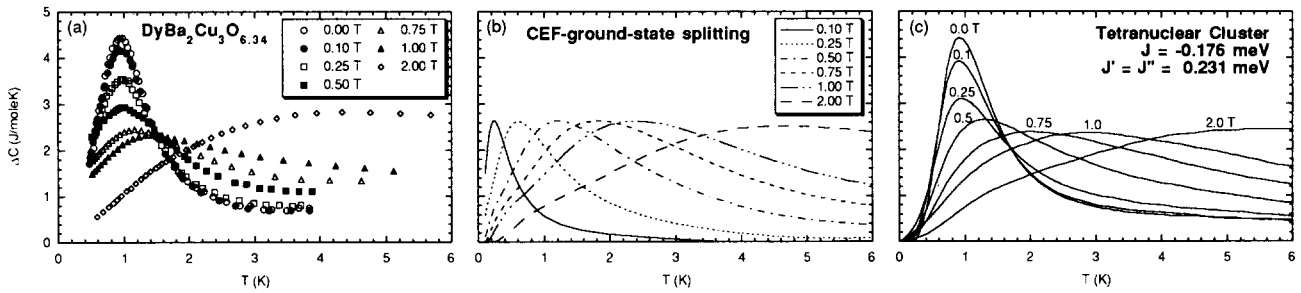

Fig. 9. The same as Fig. 7, but for $DyBa_2Cu_3O_{6.34}$ (zero-field cooled [8]). For the calculations shown in (b), due to the high single ion anisotropy of Dy^{3+}, different magnetic field directions have been used in order to obtain a reasonable powder average (the number of different directions was increased stepwise and stopped when the calculated heat capacity data converged). To obtain a powder average for (c), g was varied according to: $g_{\text{eff}}^2 = g_{\parallel}^2 \cos^2\theta + g_{\perp}^2 \sin^2\theta$; the reduction of the step size of θ was stopped when the data converged.

$$H_z = \frac{\Delta E}{Mg\mu_B} \tag{14}$$

where ΔE is the zero-field splitting between the two levels and M is the magnetic quantum number. Close to the crossing point, the two singlets form a quasi-doublet, which decreases the entropy change associated with the magnetic coupling according to eqn. (1). The less pronounced than expected decrease in the maximum of the measured specific heat is most likely due to the fact that these crossing points differ considerably for clusters of different sizes, and, therefore, a mixture of many different clusters of different sizes will smear out this dip. Certainly, including only magnetic fields in the z-direction is an oversimplification, even if the system is almost isotropic. Furthermore, measurements on these superconducting samples, are complicated by incomplete field penetration and inhomogeneity of the magnetic field. But despite all the simplifications, the cluster model describes the qualitative behavior with and without applied magnetic field rather well, certainly much better than just the doublet splitting of the CEF ground state or a long-range antiferromagnet in a magnetic field, where a decrease in T_N is expected (such a behavior is observed for the fully oxidized and the fully reduced Nd123x sample and for the fully oxidized Dy123x sample [8]).

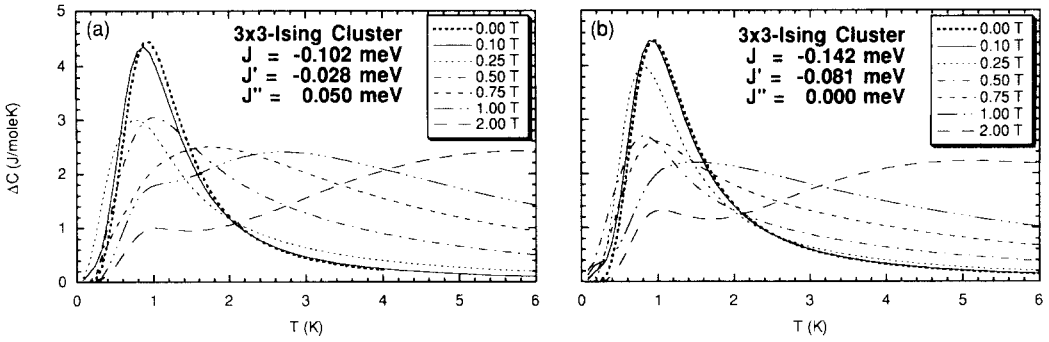

Fig. 10. Calculation of the specific heat of a 3×3-Ising cluster in a magnetic field for two different sets of exchange parameters. The powder average was obtained by use of the relation $g_{eff}^2 = g_{\parallel}^2 cos^2\theta$.

Finally, the specific heat as a function of an external magnetic field for the 3×3-Ising cluster is shown in Fig. 10. The same exchange integrals as for the zero field fits in Fig. 5 were used. Both sets of parameters provide about the same agreement with the zero field data, but fail to reproduce the qualitative behavior in a field as well as the Heisenberg cluster model does. There exist no inelastic neutron data for the CEF splitting of the oxygen deficient Dy123x; therefore, it is not clear whether the degree of anisotropy changes significantly by reducing the oxygen content, which would then favor the Heisenberg model. The restriction to fields along the c-axis and to a relatively small cluster could be another explanation.

In conclusion, we have been able to explain the origin of the magnetic specific heat of superconducting Nd123x and Dy123x in an intermediate oxygen range and of fully oxidized Nd1237 doped with Nd at the Ba site. All of these samples reveal a magnetic anomaly in the specific heat expected for a magnetic cluster system. The measured specific heat as a function of an external magnetic field also supports the cluster model approach. Including several clusters of different sizes whose formation is temperature dependent would certainly improve the agreement with the data, but in addition would increase the number of free parameters. Further measurements and other techniques (*e.g.* inelastic neutron scattering or EPR) will be needed in the future to clarify this aspect. Nevertheless, the most important question concerning the origin of the mechanism behind the decay of the long-range magnetic ordering into small magnetic clusters by only slightly changing the charge carrier density will remain unanswered.

Acknowledgment

One of us (P.A.) was supported by a fellowship from the Swiss Science Foundation. This work was supported by the U.S. Department of Energy under Grant No. DE-FG03-86ER45230.

References

1 M. Buchgeister, W. Hiller, S.M. Hosseini, K. Kopitzki and D. Wagener, in R. Niclosky (ed.), *Proc. Int. Conf. on Transport Properties of Superconductors*, Rio de Janeiro, Brazil, 1990, World Scientific, Singapore, 1990, 511 pp.
2 K.N. Yang, J.M. Ferreira, B.W. Lee, M.B. Maple, W.-H. Li, J.W. Lynn and R.W. Erwin, *Phys. Rev. B, 40* (1989) 10963.
3 Y. Nakazawa, M. Ishikawa and T. Takabatake, *Physica B, 148* (1987) 404.
4 B.W. Lee, J.M. Ferreira, S. Ghamaty, K.N. Yang and M.B. Maple, in J.L. Moran-Lopez and I.K. Schuller (ed.), *Proc. Conf. on Oxygen Disorder Effects in High-T_c Superconductors*, Triest, Italy, 1989, Plenum, New York, 1990, 151 pp.
5 B.W. Lee, *Ph. D. Thesis*, University of California, San Diego, 1990, unpublished.
6 B. W. Lee, S. Ghamaty, G. Nieva, P. Allenspach and M. B. Maple, *Phys. Rev. B,* (1993) submitted.
7 P. Allenspach, B.W. Lee, D. Gajewski, M.B. Maple, S.I. Yoo and M.J. Kramer, *J. Appl. Phys., 73* (1993) 6317.
8 P. Allenspach, B.W. Lee, D. Gajewski, M.B. Maple, G. Nieva, S.I. Yoo, M.J. Kramer, R.W. McCallum and L. Ben-Dor, unpublished.
9 P. Fischer, B. Schmid, P. Brüesch, F. Stucki and P. Unternährer, *Z. Phys. B, 74* (1989) 183.
10 T.W. Clinton, J.W. Lynn, B.W. Lee, M. Buchgeister and M.B. Maple, *J. Appl. Phys., 73* (1993) 6320.
11 J.W. Lynn, T.W. Clinton, W-H. Li, R.W. Erwin, J.Z. Liu, K. Vandervoort and R.N. Shelton, *Phys. Rev. Lett., 63* (1989) 2606.
12 G.L. Goldman and L. Soderholm, *Physica C, 171* (1990) 528.
13 P. Fischer, K. Kakurai, M. Steiner, K.N. Clausen, B. Lebech, F. Hulliger, H.R. Ott, P. Brüesch and P. Unternährer, *Physica C, 152* (1988) 145.
14 T.W. Clinton, J.W. Lynn, J.Z. Liu, Y.X. Jia and R.N. Shelton, *J. Appl. Phys., 70* (1991) 5751.
15 T.W. Clinton, *Ph. D. Thesis*, University of Maryland, 1992, unpublished.
16 A.H. Moudden, P. Schweiss, B. Hennion, P.M. Gering, G. Shirane and Y. Hidaka, *Physica C, 185–189* (1991) 1167.
17 P. Allenspach, J. Mesot, U. Staub, A. Furrer, H. Blank, H. Mutka, R. Osborn, A.T. Taylor, H. Maletta, M.J. Kramer, S.-I. Yoo, E. Kaldis, J. Karpinski and S. Rusiecki, *Physica B, 180&181* (1992) 389.
18 R.L. Carlin, *Magnetochemistry*, Springer-Verlag, Berlin, 1986.
19 U. Fano and G. Racah, *Irreducible Tensorial Sets*, Academic Press, New York, 1959.

20 E.P. Wigner, *Group Theory and its Application to the Quantum Mechanics of Atomic Spectra*, Academic Press, New York, 1959.
21 A. Furrer, Habilitation, ETH Zurich, 1978, unpublished.
22 P. Allenspach, A. Furrer and F. Hulliger, *Phys. Rev. B, 39* (1989) 2226; the anisotropic g factors on p. 2230 are too small by a factor of two.
23 B. Rössli, P. Fischer, U. Staub, M. Zölliker and A. Furrer, unpublished .
24 V.P. D'yakonov, E.E. Zubov, G.G. Levchenko, V.I. Markovich, I.M. Fita and N.A. Doroshenko, *Sov. Phys. Solid State, 33* (1991) 1848.
25 A.B. MacIsaac, J.P. Whitehead, K. De'Bell and K. Sowmya Narayanan, *Phys. Rev. B, 46* (1992) 6387.